Modal synthesis applied to a Reissner mixed plate finite element dynamic model

Pierre Garambois, Sébastien Besset, Louis Jezequel

Modal synthesis applied to a Reissner mixed plate finite element dynamic model

P. Garambois[1,a] , S. Besset[1,b], and L. Jezequel[1,c]
[1]Laboratoire de Tribologie et Dynamique des Systèmes, UMR CNRS 5513,
Ecole Centrale de Lyon, 36 avenue Guy de Collongue 69134 Ecully Cedex, France
{[a]pierre.garambois, [b]sebastien.besset, [c]louis.jezequel}@ec-lyon.fr

ABSTRACT: This paper deals with the application of component mode synthesis on thick and thin plate finite element model, built with a Reissner mixed formulation. The Reissner mixed formulation is a structural mechanical formulation mostly used in plate problems that uses both displacement and generalized stress variables. Thus, the access to the stress in the plate is easier than with a primal method. The Mindlin theory for thick plates, permits to take into consideration shearing phenomenon inside the plate, whereas the Kirchoff-Love for thin plates only deals with bending and twisting phenomenons. The Reissner-mixed and primal models show the exact same results, both for Mindlin and Kirchoff-Love theory. Nevertheless, the Kirchoff-Love mixed model shows a much better convergence than the Mindlin mixed model for thick plates.
The inconvenience of a mixed model, whatever the chosen plate theory is, is the numerical size of the finite element model that is much bigger. That's the reason why we use modal synthesis to reduce our model. The idea is to build our model with both primal and mixed formulation at the same time. Then we reduce the mixed model using a sub-structuring method and bases composed of "fixed interface modes" obtained from a Craig & Bampton method applied on the primal model. That method also shows a good convergence and permits us to reduce significantly the numerical size of our model on a certain frequency band, keeping the advantages of the Reissner mixed model.

KEY WORDS: Reissner, Mindlin, Kirchoff-Love, plate, mixed formulation, finite element, sub-structuring, vibrations.

1 INTRODUCTION

Most of the finite element plate models used in industry are based on a dynamic primal formulation. They are fast and efficient, but they need an extra calculation and integration to get the strains and thus the constrains. Another point of view developed by Reissner [1] aims at defining a new Lagrangian using both displacement fields, and generalized stress fields, called Reissner mixed function. Thus, developing this function and discretising the displacements and generalized stress fields, we obtaine a Reissner mixed finite element formulation with displacement and stress fields parameters. That method has already been used for static problems [2] [3] and more rarely for dynamic problems [4]. Most of the time, the Reissner mixed formulation is used for Mindlin thick plate theory. In this paper, we develop a Reissner mixed formulation both for thick Mindlin plate and thin Kirchoff-Love plate.

An inconvenient of the mixed formulation is the numerical size of the problems, due to the addition of generalized stress fields parameters to the displacements fields parameters of the primal method. Many sub-structuring method exist to reduce primal finite element such as "fixed interface mode" method (Craig & Bampton method [5]), free mode method (Mac Neal method [6]) and boundary mode method (Balmes method [7]). In this paper, the idea is to use those methods applied on the primal model to build a new reduced base for the sub-structured mixed model.

First of all, the article talks about a Reissner mixed variational dynamic formulation of finite element for Mindlin thick plates and set the conditions of the following finite element model. Then a Reissner-Kirchoff-Love model is also studied. Afterwards, we study the convergence of the two mixed models. In the fifth part, we deal with the application of component mode synthesis on the finite element mixed model, based on "fixed interface modes", obtained through a Craig & Bampton method applied on the primal plate problem. In the last part, we show the convergence of our problem on a simple example and the main results.

2 VARIATIONAL FORMULATION OF REISSNER MIXED FINITE ELEMENT BASED ON THICK MINDLIN PLATE

2.1 The Reissner mixed formulation

The Reissner mixed function is given by:

$$\Pi_{RD} = \iiint_V -\sigma_{\mathbf{ij}}\mathbf{e_{ij}} + \frac{1}{2}\sigma_{\mathbf{ij}}\mathbf{S_{ijkl}}\sigma_{\mathbf{kl}} + \boldsymbol{b_i u_i} + \frac{1}{2}\rho\boldsymbol{\dot{u}_i^2}\ \mathrm{dV} \tag{1}$$

considering $\sigma_{\mathbf{ij}}$ the generalized stress, $\mathbf{e_{ij}}$ the strain, $\boldsymbol{u_i}$ the displacement, $\boldsymbol{b_i}$ the body force, ρ the volumic mass and $\mathbf{S_{ijkl}}$ the elastic compliance matrix. We consider 3 main fields in the function:

- Mixed strain energy: $\sigma_{\mathbf{ij}}\mathbf{e_{ij}} - \frac{1}{2}\sigma_{\mathbf{ij}}\mathbf{S_{ijkl}}\sigma_{\mathbf{kl}}$
- Body force work: $\boldsymbol{b_i u_i}$
- Kinetic energy: $\frac{1}{2}\rho\boldsymbol{\dot{u}_i^2}$

2.2 Definition of the Mindlin theory

The displacement is given by:

$$\boldsymbol{u_i} = \begin{Bmatrix} w \\ \theta_x \\ \theta_y \end{Bmatrix} \tag{2}$$

considering w the transverse displacement, θ_x and θ_y the normal rotation around the -x and -y axis. The three displacement fields are independent in the Mindlin thick plate theory whilst the rotations depend on the transverse displacement in the Kirchoff-Love theory. Thus, the shearing phenomenon doesn't exist in that theory which simplify a lot our system and gives us smaller matrix sizes and so reduce the computational time.

The strain is given by:

$$\boldsymbol{e_{ij}} = \begin{Bmatrix} \epsilon_{xx} \\ \epsilon_{yy} \\ \gamma_{xy} \\ \gamma_{xz} \\ \gamma_{yz} \end{Bmatrix} = \mathbf{D}\,\boldsymbol{u_i} \tag{3}$$

where $\mathbf{D}$ is the following operator:

$$\mathbf{D} = \begin{Bmatrix} 0 & 0 & \frac{\partial}{\partial x} \\ 0 & -\frac{\partial}{\partial y} & 0 \\ 0 & \frac{\partial}{\partial x} & \frac{\partial}{\partial y} \\ \frac{\partial}{\partial x} & 0 & 1 \\ \frac{\partial}{\partial y} & -1 & 0 \end{Bmatrix} \tag{4}$$

The generalized stress field is given by:

$$\boldsymbol{\sigma_{ij}} = \begin{Bmatrix} M_x \\ M_y \\ M_{xy} \\ Q_x \\ Q_y \end{Bmatrix} \tag{5}$$

where $\{M_x, M_y, M_{xy}\}^T$ represents the bending and twisting moments and $\{Q_x, Q_y\}^T$ represents the transverse shear force.

The elastic compliance matrix is given by:

$$\mathbf{S_{ijkl}} = \begin{Bmatrix} \frac{12}{Et^3} & -\frac{12\nu}{Et^3} & 0 & 0 & 0 \\ -\frac{12\nu}{Et^3} & \frac{12}{Et^3} & 0 & 0 & 0 \\ 0 & 0 & \frac{24(1+\nu)}{Et^3} & 0 & 0 \\ 0 & 0 & 0 & \frac{2,4(1+\nu)}{Et} & 0 \\ 0 & 0 & 0 & 0 & \frac{2,4(1+\nu)}{Et} \end{Bmatrix} \tag{6}$$

where E is the Young Modulus, t is the thickness of the plate element and ν is the Poisson ratio.

The positive directions of the generalized stress field are shown in Figure 1.

2.3 Interpolation of nodal displacement in element

We assume that w, θ_x and θ_y, for a 4-node quadrilateral element, are interpolated in terms of nodal displacements

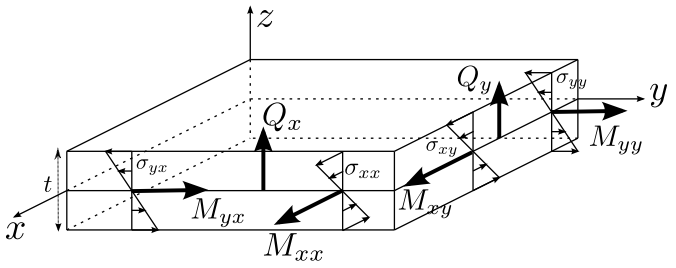

Figure 1. Bending and twisting moment and transverse shear force

$\{w_i \quad \theta_{xi} \quad \theta_{yi}\}$ (i = 1,2,3,4), as follows:

$$w(x,y) = \sum_{i=1}^{4} N_i(x,y) w_i \tag{7}$$

$$\theta_x(x,y) = \sum_{i=1}^{4} N_i(x,y) \theta_{xi} \tag{8}$$

$$\theta_y(x,y) = \sum_{i=1}^{4} N_i(x,y) \theta_{yi} \tag{9}$$

Which gives us:

$$\boldsymbol{u_i} = \begin{Bmatrix} w \\ \theta_x \\ \theta_y \end{Bmatrix} = \mathbf{N}\boldsymbol{U} \tag{10}$$

Chosing a 4-node quadrilateral element, the shape functions have 4 conditions and thus can be quadratic as follows:

$$N_i(x,y) = a_i + b_i x + c_i y + d_i xy \tag{11}$$

That condition is essential to observe shearing phenomenon.

2.4 Interpolation of stress

We assume that each field of the generalized stress is interpolated with linear function but does not depend on the nodal values, which gives a large choice of possibilities when choosing the functions. Thus, each generalized stress is interpolated with 3 parameters β, as follows:

$$\boldsymbol{\sigma_{ij}} = \begin{Bmatrix} M_x \\ M_y \\ M_{xy} \\ Q_x \\ Q_y \end{Bmatrix} = \mathbf{P}\boldsymbol{\beta}$$

$$\boldsymbol{\sigma_{ij}} = \begin{Bmatrix} 1 & x & y & 0 & 0 & 0 & 0 & 0 & 0 & ... \\ 0 & 0 & 0 & 1 & x & y & 0 & 0 & 0 & ... \\ 0 & 0 & 0 & 0 & 0 & 0 & 1 & x & y & ... \\ 0 & 0 & 0 & 0 & 0 & 0 & 0 & 0 & 0 & ... \\ 0 & 0 & 0 & 0 & 0 & 0 & 0 & 0 & 0 & ... \end{Bmatrix} \begin{Bmatrix} \beta_1 \\ \beta_2 \\ . \\ . \\ \beta_{15} \end{Bmatrix} \tag{12}$$

Those choices give us a total of 27 parameters per element matrix, as we have 12 displacement paremeters U and 15 generalized stress parameters β.

2.5 *Variational function and mixed finite element formulation*

$$\Pi_{RD} = \iiint_V -\sigma_{\mathbf{ij}}\mathbf{e_{ij}} + \frac{1}{2}\sigma_{\mathbf{ij}}\mathbf{S_{ijkl}}\sigma_{\mathbf{kl}} + \boldsymbol{b_i u_i} + \frac{1}{2}\rho\boldsymbol{\dot{u}_i^2}\,\mathrm{dV}$$

$$\Pi_{RD} = \iint_S \frac{1}{2}(\mathbf{N}\dot{\boldsymbol{U}})^T\mathbf{m}(\mathbf{N}\dot{\boldsymbol{U}}) - (\mathbf{P}\boldsymbol{U})^T(\mathbf{D}\mathbf{N}\boldsymbol{U}) + \frac{1}{2}(\mathbf{P}\boldsymbol{\beta})^T\mathbf{S}(\mathbf{P}\boldsymbol{\beta})\,\mathrm{dS} + \iint_V b_i\boldsymbol{U}\mathrm{dS} \tag{13}$$

where

$$\mathbf{m} = \rho\begin{Bmatrix} t & 0 & 0 \\ 0 & \frac{t^3}{12} & 0 \\ 0 & 0 & \frac{t^3}{12} \end{Bmatrix} \tag{14}$$

and ρ is the density.
The matrix development gives us:

$$\Pi_{RD} = \frac{1}{2}\dot{\boldsymbol{U}}^T\mathbf{M}\dot{\boldsymbol{U}} - \boldsymbol{\beta}^T\mathbf{G}\boldsymbol{U} - \boldsymbol{\beta}^T\mathbf{H}\boldsymbol{\beta} + \boldsymbol{F}^T\mathbf{U} \tag{15}$$

where

$$\mathbf{M} = \iint_S \mathbf{N}^T\mathbf{m}\mathbf{N}\mathrm{dS} \tag{16}$$

$$\mathbf{G} = \iint_S \mathbf{P}^T\mathbf{D}\mathbf{N}\mathrm{dS} \tag{17}$$

$$\mathbf{H} = \iint_S -\mathbf{P}^T\mathbf{S}\mathbf{P}\mathrm{dS} \tag{18}$$

and $\boldsymbol{F}$ is the force vector applied to the mesh nodes.
Then we have:

$$\begin{Bmatrix} \mathbf{M} & \mathbf{0} \\ \mathbf{0} & \mathbf{0} \end{Bmatrix}\begin{Bmatrix} \ddot{\boldsymbol{U}} \\ \ddot{\boldsymbol{\beta}} \end{Bmatrix} + \begin{Bmatrix} \mathbf{0} & \mathbf{G}^T \\ \mathbf{G} & \mathbf{H} \end{Bmatrix}\begin{Bmatrix} \boldsymbol{U} \\ \boldsymbol{\beta} \end{Bmatrix} = \begin{Bmatrix} \boldsymbol{F} \\ \mathbf{0} \end{Bmatrix} \tag{19}$$

3 VARIATIONAL FORMULATION OF REISSNER MIXED FINITE ELEMENT BASED ON THIN KIRCHOFF-LOVE PLATE

3.1 *The Reissner mixed formulation*

The Reissner mixed function is still given by:

$$\Pi_{RD} = \iiint_V -\sigma_{\mathbf{ij}}\mathbf{e_{ij}} + \frac{1}{2}\sigma_{\mathbf{ij}}\mathbf{S_{ijkl}}\sigma_{\mathbf{kl}} + \boldsymbol{b_i u_i} + \frac{1}{2}\rho\boldsymbol{\dot{u}_i^2}\,\mathrm{dV} \tag{20}$$

considering $\sigma_{\mathbf{ij}}$ the generalized stress, $\mathbf{e_{ij}}$ the strain, $\boldsymbol{u_i}$ the displacement, $\boldsymbol{b_i}$ the body force, ρ the volumic mass and $\mathbf{S_{ijkl}}$ the elastic compliance matrix.

3.2 *Definition of the Kirchoff-Love theory*

The displacement is given by:

$$\boldsymbol{u_i} = \begin{Bmatrix} w \\ \theta_x \\ \theta_y \end{Bmatrix} = \begin{Bmatrix} w \\ \frac{\partial w}{\partial y} \\ -\frac{\partial w}{\partial x} \end{Bmatrix} \tag{21}$$

considering w the transverse displacement, $\theta_{\mathbf{x}}$ and $\theta_{\mathbf{y}}$ the normal rotation around the -x and -y axis. The theory of Kirchoff-Love assume that the 2 rotations $\theta_{\mathbf{x}}$ and $\theta_{\mathbf{y}}$ depend on the transverse displacement $\mathbf{w}$.

The strain is given by:

$$\boldsymbol{e_{ij}} = \begin{Bmatrix} \epsilon_{xx} \\ \epsilon_{yy} \\ \gamma_{xy} \end{Bmatrix} = \mathbf{D}\,\boldsymbol{u_i} \tag{22}$$

where $\mathbf{D}$ is the operator

$$\mathbf{D} = \begin{Bmatrix} 0 & 0 & \frac{\partial}{\partial x} \\ 0 & -\frac{\partial}{\partial y} & 0 \\ 0 & \frac{\partial}{\partial x} & \frac{\partial}{\partial y} \end{Bmatrix} \tag{23}$$

The generalized stress field is given by:

$$\boldsymbol{\sigma_{ij}} = \begin{Bmatrix} M_x \\ M_y \\ M_{xy} \end{Bmatrix} \tag{24}$$

where $\{M_x, M_y, M_{xy}\}^T$ represents the bending and twisting moments. The transverse shearing force is not taken into consideration using the Kirchoff-Love theory.

The elastic compliance matrix is given by:

$$\mathbf{S_{ijkl}} = \begin{Bmatrix} \frac{12}{Et^3} & -\frac{12\nu}{Et^3} & 0 \\ -\frac{12\nu}{Et^3} & \frac{12}{Et^3} & 0 \\ 0 & 0 & \frac{24(1+\nu)}{Et^3} \end{Bmatrix} \tag{25}$$

3.3 *Interpolation of nodal displacement in element*

We assume that w, θ_x and θ_y, for a 3-node triangular element, are interpolated in terms of nodal displacements $\{w_i \quad \theta_{xi} \quad \theta_{yi}\}$ (i = 1,2,3), as follows:

$$w(x,y) = \sum_{i=1}^{3} N_i(x,y)w_i \tag{26}$$

$$\theta_x(x,y) = \sum_{i=1}^{3} \frac{\partial N_i(x,y)}{\partial y}\theta_{xi} \tag{27}$$

$$\theta_y(x,y) = \sum_{i=1}^{3} -\frac{\partial N_i(x,y)}{\partial x}\theta_{yi} \tag{28}$$

Which gives us:

$$\boldsymbol{u_i} = \begin{Bmatrix} w \\ \theta_x \\ \theta_y \end{Bmatrix} = \mathbf{N}\boldsymbol{U} = \begin{Bmatrix} N_1 & N_2 & \dots & N_9 \\ \frac{\partial N_1}{\partial y} & \frac{\partial N_2}{\partial y} & \dots & \frac{\partial N_9}{\partial y} \\ -\frac{\partial N_1}{\partial x} & -\frac{\partial N_2}{\partial x} & \dots & -\frac{\partial N_9}{\partial x} \end{Bmatrix} U \tag{29}$$

Chosing a 3-node triangular element, the shape functions have 9 conditions each and thus are 3rd order polynomials as follows:

$$N_i(x,y) = a_i + b_i x + c_i y + d_i xy + e_i x^2 + f_i y^2 + g_i x^3 + h_i y^3 + i_i xy^2 \tag{30}$$

3.4 *Interpolation of stress*

As the Mindlin theory, we assume that each field of the generalized stress is interpolated with linear function and does not depend on the nodal values. Each generalized stress is interpolated with 3 parameters β, as follows:

$$\boldsymbol{\sigma_{ij}} = \begin{Bmatrix} M_x \\ M_y \\ M_{xy} \end{Bmatrix} = \mathbf{P}\boldsymbol{\beta}$$

$$\boldsymbol{\sigma_{ij}} = \begin{Bmatrix} 1 & x & y & 0 & 0 & 0 & 0 & 0 & 0 \\ 0 & 0 & 0 & 1 & x & y & 0 & 0 & 0 \\ 0 & 0 & 0 & 0 & 0 & 0 & 1 & x & y \end{Bmatrix} \begin{Bmatrix} \beta_1 \\ \beta_2 \\ . \\ . \\ \beta_9 \end{Bmatrix} \quad (31)$$

Those choices give us a total of 18 parameters per element matrix, as we have 9 displacement paremeters U and 9 generalized stress parameters β.

3.5 *Variational function and mixed finite element formulation*

As the Reissner-Mindlin theory, the matrix development of the Reissner-Kirchoff-Love theory gives us the same result as equation 19:

$$\begin{Bmatrix} \mathbf{M} & \mathbf{0} \\ \mathbf{0} & \mathbf{0} \end{Bmatrix} \begin{Bmatrix} \ddot{\boldsymbol{U}} \\ \ddot{\boldsymbol{\beta}} \end{Bmatrix} + \begin{Bmatrix} \mathbf{0} & \mathbf{G}^T \\ \mathbf{G} & \mathbf{H} \end{Bmatrix} \begin{Bmatrix} \boldsymbol{U} \\ \boldsymbol{\beta} \end{Bmatrix} = \begin{Bmatrix} \boldsymbol{F} \\ \mathbf{0} \end{Bmatrix} \quad (32)$$

4 CONVERGENCE STUDY OF THE MIXED MODEL

4.1 *Mindlin theory*

The example we study in this part is a rectangular thick plate built with Reissner-Mindlin mixed quadrangular finite elements described in the the section 2. The plate is clamped on one edge, and free on the three other edges. It is made of steel (see characteristics 1) and the thickness t of the plate is a variable of the different simulation. That example is shown in figure 2.

Table 1. Steel characteristics

Young Modulus (Pa)	2.1×10^{11}
Poisson ratio	0.33
Density ($kg.m^{-3}$)	7.5×10^3

The numerical simulations we make shows the exact same convergence for the Reissner-Mindlin mixed model and the Mindlin primal model. Nevertheless, the results obtained with the Mindlin theory for various thickness of the plate (Table 2 and Table 3) show that the convergence of the model needs a high number of elements. It appears that the characteristic size of the element needs to be at least equal or even smaller than the thickness of the plate to get acceptable results, which means that the smaller the

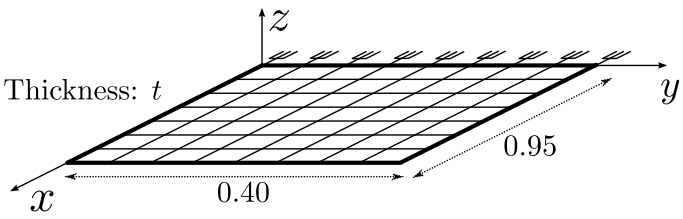

Figure 2. Rectangular thick plate built with Reissner-Mindlin quad elements

Table 2. Relative error for the first eigenfrequencies for the example 1 with $t = 0.05m$ and Reissner Mindlin mixed model

	Element size (cm)				
	9.5	4.8	3.2	2.4	1.9
Mode \ Elt	100	400	900	1600	2500
1	44.3	12.7	5.7	3.2	0.01
2	15.5	1.9	0.6	0.16	0.00
3	46.2	12.9	5.9	3.2	0.02
4	12.0	3.2	1.4	0.7	0.00
5	19.0	13.5	6.0	3.3	0.002
6	15.21	5.9	2.5	1.4	0.01
7	26.3	14.9	9.0	0.13	0.00
8	29.5	5.3	1.7	0.9	0.00
9	34.0	8.6	3.7	2.0	0.01
10	16.50	2.4	1.0	0.48	0.00

Table 3. Relative error for the first eigenfrequencies for the example 1 with $t = 0.01m$ and Reissner Mindlin mixed model

	Element size (cm)				
	2.4	1.9	1.6	1.35	1.19
Mode \ Elt	1600	2500	3600	4900	6400
1	64.2	43.7	32.4	24.2	19.1
2	8.1	5.6	4.0	2.9	2.3
3	100	44.5	32.4	32.4	19.3
4	24.9	10.3	7.3	7.3	4.2
5	100	44.2	32.2	32	19.0
6	44.5	18.06	12.7	12.8	7.4
7	35.8	20.4	17.2	17.2	13.2
8	45.6	33.9	19.3	19.3	8.7
9	46.9	26.0	8.5	5.5	3.0
10	59.6	25.3	18.0	18.0	10.4

thickness is, the smaller the elements need to be, which can cause a lot of numerical problems (mass and stiffness matrix with big numerical sizes, especially with the mixed model).

4.2 Kirchoff-Love theory

The example we study in this part is a rectangular thick plate built with Reissner-Kirchoff-Love mixed triangular finite elements described in the the section 3. The plate is clamped on one edge, and free on the three other edges. It is made of steel (see characteristics in Table 1) and the thickness t of the plate is a variable of the different simulation. That example is shown in figure 3.

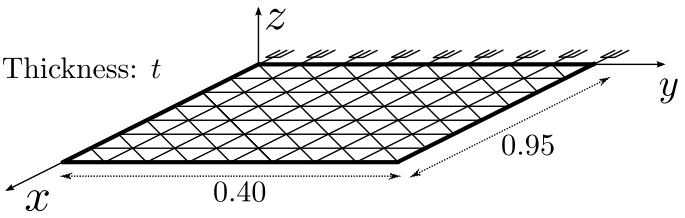

Figure 3. Rectangular thin plate built with Reissner-Kirchoff-Love triangular elements

Table 4. Relative error for the first eigenfrequencies for the example 1 with $t = 0.01m$ and Reissner Kirchoff-Love mixed model

	Element size (cm)			
	47.5	23.8	32.9	5.9
Mode \ Elt	16	64	256	1024
1	2.94	1.47	0.53	0.21
2	8.13	1.90	0.42	0.10
3	6.80	1.19	0.40	0.13
4	-	7.58	1.63	0.33
5	-	2.87	0.24	0.06
6	-	11.59	2.28	0.41
7	-	1.72	0.01	0.01
8	-	4.90	0.27	0.00
9	-	3.35	0.06	0.00
10	-	20.35	3.29	0.43

The numerical simulations we make also shows the exact same convergence for the Reissner-Kirchoff-Love mixed model and the Kirchoff primal model. Nevertheless, the results obtained with the Kirchoff-Love theory for various thickness of the plate (Table 4 and Table 5) show a significantly higher convergence than the Mindlin theory. It appears that the characteristic size of the element doesn't influence the convergence of the model, as long as we stay in small thickness, as the Kirchoff-Love theory defines.

5 MODAL REDUCTION

As described in the first sections, the numerical sizes of the Reissner-Mindlin thin plate mixed model and the Reissner-Kirchoff-Love thick plate mixed model are significantly higher than primal models using the same theories. The idea of this part is to reduce the numerical size of the model with a sub-structuring method, using "fixed interface modes" method obtained with a primal model (considering the same characcteristics and meshes). We describe this modal reduction in the following section.

Table 5. Relative error for the first eigenfrequencies for the example 1 with $t = 0.001m$ and Reissner Kirchoff-Love mixed model

	Element size (cm)			
	47.5	23.8	32.9	5.9
Mode \ Elt	16	64	256	1024
1	3.16	2.11	1.05	0.00
2	8.14	1.67	0.42	0.00
3	6.68	1.17	0.33	0.00
4	43.16	7.55	1.63	0.32
5	24.84	2.86	0.24	0.18
6	-	11.56	2.26	0.38
7	-	1.77	0.01	0.00
8	-	4.85	0.26	0.00
9	-	3.60	0.29	0.06
10	-	20.36	3.72	0.41

5.1 Projection of displacements: Craig & Bampton Method

The Craig & Bampton Method is a sub-structuring primal method that separates, for each sub-structure a, boundary DOF's $\boldsymbol{U}_j^a$ and internal DOF's $\boldsymbol{U}_i^a$. It projects the initial DOF's of the sub-structure a on a new smaller base composed of the same boundary DOF's $\boldsymbol{U}_j^a$ (we also call them "physical DOF's") and truncated modal DOF's $\boldsymbol{\eta}_{eU}^a$ (which will be DOF's only for the displacements), as follows:

$$\begin{Bmatrix} \boldsymbol{U}_i^a \\ \boldsymbol{U}_j^a \end{Bmatrix} = \begin{Bmatrix} \boldsymbol{\Phi}_{eU}^a & \boldsymbol{\Psi}_{ij}^a \\ \mathbf{0} & \mathbf{I} \end{Bmatrix} \begin{Bmatrix} \boldsymbol{\eta}_{eU}^a \\ \boldsymbol{U}_j^a \end{Bmatrix} \tag{33}$$

where $\boldsymbol{\Phi}_{eU}^a$ is a truncated base composed of eigenmodes of the structure a assuming that the boundary nodes are held fixed (concerning the displacement fields), $\boldsymbol{\Psi}_{ij}^a$ is the attachment modes matrix $\boldsymbol{\Psi}_{ij}^a = -\mathbf{K}_{ii}^a(\mathbf{K}_{ij}^a)^{-1}$.

5.2 Projection of generalized stress field: Craig & Bampton Method on the stress

For each sub-structure a, in order to access to the generalized stress field parameters, we use the relation between $\boldsymbol{\beta}^a$ and $\boldsymbol{U}^a$: $\boldsymbol{\beta}^a = -(\mathbf{H}^a)^{-1}\mathbf{G}^a\boldsymbol{U}^a$. We also use a Craig & Bampton method to access to the displacement fields $\boldsymbol{U^a}$ corresponding to the generalized stress fields $\boldsymbol{\beta^a}$, as follows:

$$\beta^a = \begin{Bmatrix} \mathbf{P}^a \begin{Bmatrix} \boldsymbol{\Phi}_{eU}^a \\ 0 \end{Bmatrix} & \mathbf{P}^a \begin{Bmatrix} \boldsymbol{\Psi}_{ij}^a \\ \mathbf{I} \end{Bmatrix} \end{Bmatrix} \cdot \begin{Bmatrix} \boldsymbol{\eta}_{e\beta}^a \\ \boldsymbol{U}_j^a \end{Bmatrix} \tag{34}$$

where $\mathbf{P}^a = -(\mathbf{H}^a)^{-1}\mathbf{G}^a$, $\boldsymbol{\eta}_{e\beta}^a$ are the modal DOF's for the generalized stress fields and $\boldsymbol{\Phi}_{e\beta}^a$ is a truncated base composed of eigenmodes of the structure a assuming that

the boundary nodes are held fixed and concerning the generalized stress fields.

5.3 *Reduction of a sub-structure*

Considering the sections 5.1 and 5.2, the reduction of the whole sub-structure a is given by:

$$\begin{Bmatrix} \boldsymbol{U}_i^a \\ \boldsymbol{U}_j^a \\ \boldsymbol{\beta}^a \end{Bmatrix} = \begin{Bmatrix} \boldsymbol{\Phi}_{e\beta}^a & \mathbf{0} & \boldsymbol{\Psi}_{ij}^a \\ \mathbf{0} & \mathbf{0} & \mathbf{I} \\ \mathbf{0} & \mathbf{P}^a \begin{Bmatrix} \boldsymbol{\Phi}_{e\beta}^a \\ \mathbf{0} \end{Bmatrix} & \mathbf{P}^a \begin{Bmatrix} \boldsymbol{\Psi}_{ij}^a \\ \mathbf{I} \end{Bmatrix} \end{Bmatrix} \begin{Bmatrix} \boldsymbol{\eta}_{eU}^a \\ \boldsymbol{\eta}_{e\beta}^a \\ \boldsymbol{U}_j^a \end{Bmatrix} \tag{35}$$

5.4 *Assembly*

We assemble two the sub-structures a and b considering $\boldsymbol{U}_j^a = \boldsymbol{U}_j^b = \boldsymbol{U}_i$, which gives us the following form:

$$\begin{Bmatrix} \boldsymbol{U}_i^a \\ \boldsymbol{U}_j \\ \boldsymbol{U}_i^b \\ \boldsymbol{\beta}^a \\ \boldsymbol{\beta}^b \end{Bmatrix} = \mathbf{T} \begin{Bmatrix} \boldsymbol{\eta}_{eU}^a \\ \boldsymbol{\eta}_{e\beta}^a \\ \boldsymbol{U}_j \\ \boldsymbol{\eta}_{eU}^b \\ \boldsymbol{\eta}_{e\beta}^b \end{Bmatrix} \tag{36}$$

where

$$T = \begin{Bmatrix} \boldsymbol{\Phi}_{eU}^a & \mathbf{0} & \boldsymbol{\Psi}_{ij}^a & \mathbf{0} & \mathbf{0} \\ \mathbf{0} & \mathbf{0} & \mathbf{I} & \mathbf{0} & \mathbf{0} \\ \mathbf{0} & \mathbf{0} & \boldsymbol{\Psi}_{ij}^b & \boldsymbol{\Phi}_{eU}^a & \mathbf{0} \\ \mathbf{0} & \mathbf{P}^a \begin{Bmatrix} \boldsymbol{\Phi}_{e\beta}^a \\ \mathbf{0} \end{Bmatrix} & \mathbf{P}^a \begin{Bmatrix} \boldsymbol{\Psi}_{ij}^a \\ \mathbf{I} \end{Bmatrix} & \mathbf{0} & \mathbf{0} \\ \mathbf{0} & \mathbf{P}^b \begin{Bmatrix} \boldsymbol{\Psi}_{ij}^b \\ \mathbf{I} \end{Bmatrix} & \mathbf{0} & \mathbf{0} & \mathbf{P}^b \begin{Bmatrix} \boldsymbol{\Phi}_{e\beta}^b \\ \mathbf{0} \end{Bmatrix} \end{Bmatrix} \tag{37}$$

6 CONVERGENCE STUDY OF THE REDUCTION

6.1 *Example*

This section focus on the convergence of the Reissner mixed model using the method described in section 5 with the theory of Kirchoff-Love, depending on the number of modes "fixed interface modes" kept in the truncation both for displacement fields and generalized stress fields. The example used in this part is composed of two different plates, meshed with Reissner-Kirchoff-Love triangular mixed elements described in section 3. It is made of steel (see characteristics in table 1) and we choose a thickness of $1e^{-3}m$. That example is shown in figure 4.

The first plate is clamped on one edge (102 DOF's clamped) and composed of 414 elements and 5064 DOF's (of which 1338 are displacement parameters and 3726 stress parameters), whereas the second plate is composed of 510 elements and 6294 DOF's (of which 1722 are displacement parameters and 4572 stress parameters). The jonction is composed of 102 boundary DOF's.

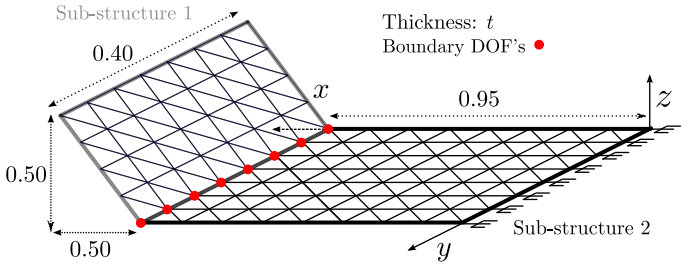

Figure 4. Rectangular thick plate built with Reissner-Mindlin quad elements

6.2 *Results*

The results are shown in figure 5. We calculate the FRF of the test structure with different modal synthesis applied on each sub-structure. In each case, the number of displacement field modes and generalized stress field modes are the same for the sub-structure 1 and the sub-structure 2. The results show a good convergence, even with a low number of modes.

It appears that choosing 20 displacement field modes and 20 generalized stress field modes permits a good convergence of the model until $100Hz$ (27 first modes observable), whereas choosing 10 modes both for displacement field and generalized stress field give good results until $70Hz$ (20 first modes observable) and 5 modes until $35Hz$ (12 first modes observable). Those results confirm the choice of using the "Craig & Bampton method" both for displacement field and generalized stress field, and permit to greatly decrease the numerical size of the mixed model (see table 6). The figure 6 shows the Von Mises stress distribution in the plate for the 12^{th} mode ($f = 331Hz$) and the shape of the mode for our example, obtained with a modal synthesis with 20 displacement field modes and 20 generalized stress field modes.

Table 6. Maximum frequency of convergence and number of observable modes in function of the number of modes chosen for the truncation

DOF's	Displacement & stress modes	Maximum frequencies (Hz)	Observed modes
11256	Non-reduced model		
502	200 & 200	1700	>200
182	20 & 20	100	27
142	10 & 10	70	20
122	5 & 5	35	12

6.3 *Prospects*

Even though the convergence of our mixed reduced model appears to be quite good, others modal synthesis have been studied to decrease the number of DOF's such as free modes method [6] and interface modes method [7]. We can also change the truncation in function of the displacements or generalized stress fields and change the types of synthesis (fixed interface modes or free modes).

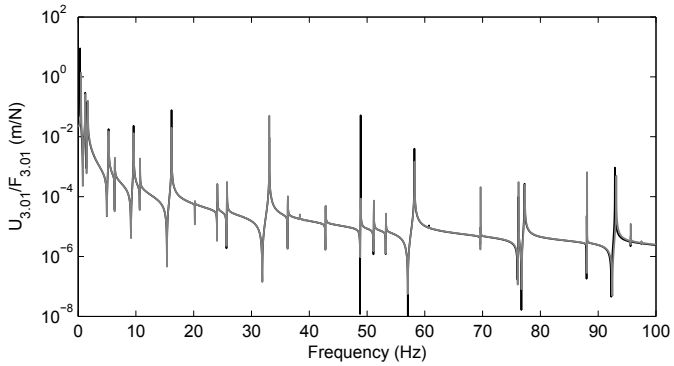

(a) 20 displacement modes & 20 stress modes for each sub-structure (black: reference / grey: reduced)

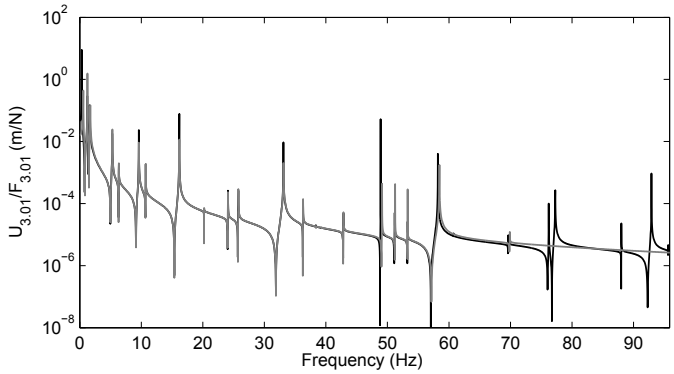

(b) 10 displacement modes & 10 stress modes for each sub-structure (black: reference / grey: reduced)

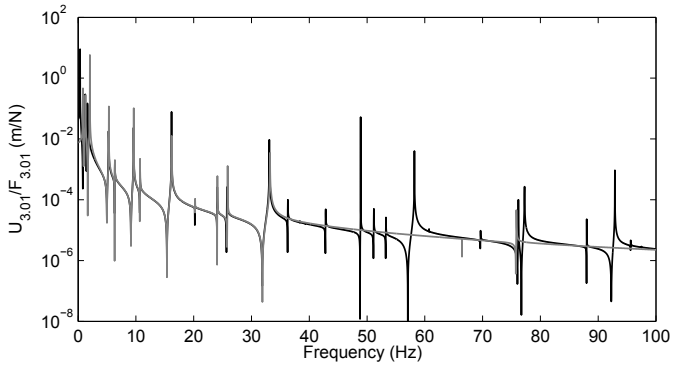

(c) 5 displacement modes & 5 stress modes for each sub-structure (black: reference / grey: reduced)

Figure 5. FRF of the test structure calculated with modal synthesis on the mixed model in function of the truncation

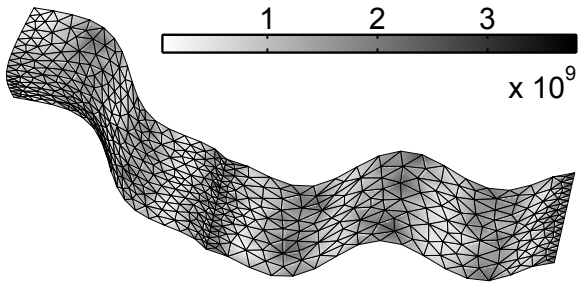

Figure 6. Von Mises stress distribution in the 2 plates for the 12^{th} mode ($f = 331Hz$) obtained with the β parameters of the model with reduction figure 5a

7 CONCLUSIONS

This article deals with a new Reissner mixed finite element plate model applied to a thick plate model (Mindlin theory) and a thin plate model (Kirchoff-Love theory). First of all, the mixed and the primal model show exactly the same convergence with the same amount of elements. Then, if we focus on the difference between thin plates theories (which considers only bending and twisting moments) and thick plates theory (which also considers transverse shear forces), the calculations we make with our code on simple examples show a significantly different convergence between the 2 theories. The Kirchoff-Love Reissner mixed model for thin plate shows a quite good convergence as it needs about 250 elements for a thickness of $t = 0.01m$ to get a good convergence ($\epsilon < 3\%$), and those results doesn't depend on the thickness. Nevertheless, the Mindlin Reissner mixed model for thick plate shows a much worse convergence as it needs about 1600 elements for a thickness of $t = 0.05m$ to get good results. Furthermore, the results with the Mindlin theory look dependent on the thickness: in fact, the smaller the thickness is, the smaller the element have to be. As a results, the same example with a thickness of $t = 0.01m$ needs more than 6400 elements to converge. As the Kirchoff-Love mixed model shows a much better convergence, even for a $0.01m$ thickness which is quite high for a plate model, we decide to choose it for the rest of the study.

The inconvenience of a mixed model, be it for Kirchoff-Love or Mindlin theory, is the numerical size of the finite element model that is much bigger as it uses parameters for the generalized stress fields and the elementary mass and stiffness matrix are bigger. That's the reason why we try use modal synthesis to reduce our model. The reduction we make aims at using modes obtained with a primal model of the same meshes and same theory, which means we build both primal and Reissner mixed assemblage at the same time for each examples. We reduce the mixed model using a sub-structuring method and bases composed of "fixed interface modes" obtained from a Craig & Bampton method. That modal synthesis, both applied on displacements and generalized stress fields parameters show a good convergence with our case (double plate with a thickness $t = 1e^{-3}m$) as we can reduce the size from about 11 000 DOF's to about 200 DOF's and still be able to observe the 30 first modes. It improves considerably the computation time and, keeps the advantages of a Reissner mixed model with access to both the displacements and generalized stresses.

AKNOWLEDGEMENT

The first author gratefully acknowledges the French Education Ministry which supports this research.

References

[1] E. Reissner. On a mixed variational theorem and on shear feformable plate theory International Journal For Numerical Methods In Engineering, 23: 193-198, 1986.

[2] Eduardo M.B.R. Pereira & Joao A.T. Freitas Numerical implementation of hybrid-mixed finite element model for Reissner-Mindlin plates Computers and Structures, 74, 323-334, 2000.

[3] Mei Duan, Yutaka Miyamoto, Shoji Iwasaki & Hideaki Deto Numerical implementation of hybrid-mixed finite element model for Reissner-Mindlin plates Finite Element in Analysis and Design, 33, 167-185, 1999.

[4] H. Nguyen-Xuan, G.R. Liu, C. Thai-Hoang & T. Nguyen-Thoi An edge-based smoothed finite element method (ES-FEM) with stabilized discrete shear gap technique for analysis of Reissner-Mindlin plates Computational Method Applied for Mechanical Engineering, 199, 471-489, 2010.

[5] R.R. Craig & Mervin C.C. Bampton. Coupling of substructures for dynamic analysis. AIAA Journal, 6(7): 1313-1319, 1968.

[6] Richard H. MacNeal. A hybrid methof of component mode synthesis. Computer and Structures, 1: 581-601, 1971.

[7] E. Balmes. Use of generalized interface degrees of freedom in component mode synthesis. Proceeding of IMAC, pages 204-210, 1996.